Does Brain Functional Connectivity Alter Across Similar Trials During Imaging Experiments?

Li Zhu and Laleh Najafizadeh

Department of Electrical and Computer Engineering, Rutgers University, Piscataway, NJ 08854

E-mail: victor.li.zhu@rutgers.edu, laleh.najafizadeh@rutgers.edu

Abstract—In a typical functional brain imaging experiment, brain activities in response to several trials are measured. Recorded signals are then averaged across similar trials for each channel/voxel to obtain time-courses associated with the task of interest. Majority of functional connectivity studies employ these averaged signals to study brain's functional connections across channels/voxels. The assumption here, however, is that functional connections among brain networks do not change across trials during the course of the experiment. In this paper, we argue that this assumption may not always hold true. Using Functional Near-Infrared Spectroscopy (fNIRS), brain activities of five healthy adults in response to modified visual oddball task are recorded. Wavelet transform coherence (WTC) is then used to assess functional connectivity by considering recordings corresponding to three scenarios: *i)* the first half of total number of similar trials, *ii)* the second half of total number similar trials, and *iii)* the entire number of similar trials. Nonparametric permutation testing is utilized to examine the statistical difference in functional connectivity when assessed in these three scenarios. Observed differences suggest that brain's functional connectivity across similar trials changes during the course of the experiment, potentially due to changes in functional connections among brain networks as a result of task repetition.

I. INTRODUCTION

The human brain, a network of 100 billion neurons [1], is known to be one of the most complex systems in nature. To date, a variety of imaging tools along with signal processing techniques, have been utilized to advance our knowledge about the mechanisms underlying the brain function. Among these techniques, studies of resting-state and task-based functional connectivity [2], aiming at identifying statistically similar behaving regions of the brain, have recently received increased attention [3]–[6]. These studies investigate how different networks in the brain (which are not necessarily anatomically connected) are functionally coupled together, and how these couplings relate to a particular process or task. Recent studies of functional connectivity in patients with neurological and psychiatric disorders [7]–[9], suggest that functional connectivity has a great potential to become a clinical tool for the early diagnosis of brain-related disorders.

To study task-based functional connectivity, first, task-related activities from different regions of the brain need to be identified. A common approach is to record brain activities of participants when they are engaged in experiments with multiple trials related to the task of interest. The recorded time-courses across similar trials are then averaged to estimate the task-related time-course for each channel/voxel. The second step is to assess the statistical dependencies between these averaged time-courses. Several similarity metrics including model-dependent measures (e.g. seed-based correlation [10]), data driven measures (e.g. independent component analysis (ICA) [11], [12]), and multiresolution analysis (e.g. wavelet transform coherence (WTC) [13]) have been used to quantify functional connections among brain regions.

One assumption in this approach is that brain's functional connections do not change during the experiment across repeated trials. However, variability in time-courses from trial to trial has been reported in previous studies [14]–[16]. To investigate changes in brain's functional connections during the course of an experiment, we study functional connectivity during three temporal segments. These segments correspond to the first half, the second half, and the entire number of similar trials. Recordings of brain activities are made using Functional Near-Infrared Spectroscopy (fNIRS). fNIRS is a promising non-invasive technique which uses light in the range of $690\ nm$ to $1000\ nm$ to measure the local changes in the cerebral concentration of oxy- (ΔHbO_2) and deoxy-hemoglobin (ΔHbR) associated with the underlying brain activities [14], [17]–[19]. Wavelet transform coherence (WTC) is used to assess statistical similarities among time-courses from different channels. Two-sample nonparametric statistical testing is then performed to compare the statistical differences in functional connectivity when assessed in the three scenarios.

This paper is organized as follows: in Section II details of the experimental procedures are provided. In Section III preprocessing steps, similarity and statistical analysis are described. Finally, results and conclusions are presented in Section IV.

II. EXPERIMENTAL PROCEDURES

Five right-handed male healthy volunteers (mean age 26.5 years, range 20-34) participated in this study after providing written informed consents. The experimental procedures were approved by the Rutgers University Institutional Review Board prior to the experiment.

The modified visual odd ball task [20] was used as the paradigm for this study. It consisted of three graphical stimuli (plus, square, circle), as shown in Fig. 1, which were presented to participants in random order. Participants were instructed to press the left button of the mouse once the target stimulus ("plus") is shown on the screen. The total number of trials was 220 stimuli, from which 30 were the target stimuli, and 190 were non-target stimuli. Each stimulus was presented for

50 ms, with inter-trial interval (ITI) of $10-12$ s. The random range for ITI was selected to minimize the periodic systemic components [21].
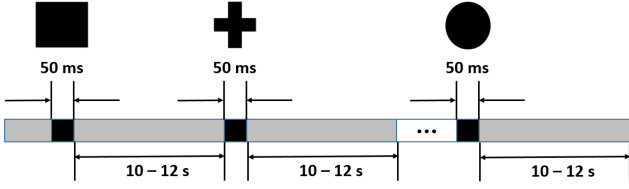

Fig. 1. Experimental paradigm for the visual odd ball task.

NIRS data were collected via *NIRx* System (NIRScout, NIRx Medical Technologies, LLC). The system included 16 sources (LED diodes) and 16 detectors, and recordings were made at a sampling rate of 10.42 Hz. Measured signals from source-detector pairs with distance of 3 mm of separation were considered, resulting in total number of 38 channels. Optodes were placed over the prefrontal and visual regions of the cortex. Each source consisted of two LED diodes (760 nm and 830 nm).

III. METHODS

A. Preprocessing

The modified Beer Lambert law (MBLL) [22] was used to extract ΔHbO_2 and ΔHbR signals. The extracted signals were detrended, segmented (according to trials) and baseline-corrected. To detect trials with artifacts, trials with either rapid changes [23] or with outliers (based on statistical distribution) were detected and removed from further analysis.

B. Wavelet Transform Coherence

Wavelet transform coherence (WTC) enables the analysis of the coherence and phase lag between two time series in both time and frequency domains [13], [24]–[26], and therefore, can be used as a measure of functional connections between recorded signals. The Morlet wavelet (with $\omega_0 = 6$), was used in this study as the wavelet function [13], [27]:

$$\psi_0(\eta) = \pi^{-1/4} e^{i\omega_0\eta} e^{-\eta^2/2}, \qquad (1)$$

where ω_0 and η are the selected frequency and time resolution, respectively. For signal x_n with length N, its continuous wavelet transform is defined as the convolution of x_n with the scaled and normalized wavelet:

$$W_{x_n}(n,s) = \sqrt{\frac{\Delta t}{s}} \sum_{m=1}^{N} x_m \psi_0[(m-n)\frac{\Delta t}{s}], \qquad (2)$$

where the parameter n is the time index, s is the scale which is used to stretch the wavelet in time, Δt is the size of uniform time step. The wavelet transform coherence (WTC) is defined as [28]:

$$R^2_{x_n,y_n}(n,s) = \frac{|S(s^{-1}W_{x_n,y_n}(n,s))|^2}{S(s^{-1}|W_{x_n}(n,s)|^2) \cdot S(s^{-1}|W_{y_n}(n,s)|^2)}. \qquad (3)$$
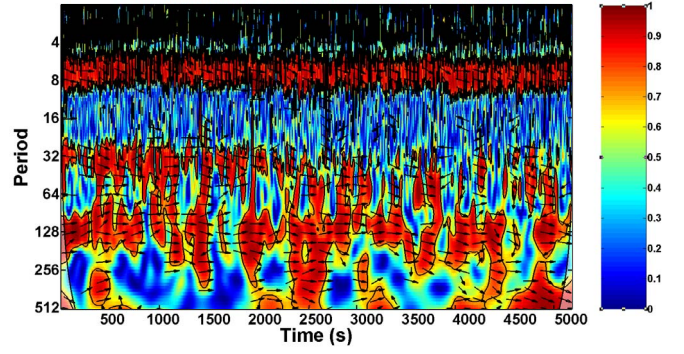

Fig. 2. Wavelet transform coherence between ΔHbO_2 signal recorded from Channel 1 and ΔHbO_2 signal recorded from Channel 26. The upper high coherence band around period of 8 (frequency of 0.77 Hz) corresponds to the cardiac activity. The lower high coherence band between the period of 104 and 125 (frequency of 0.08 Hz and 0.1 Hz respectively) relates to the task.

In (3), S represents smoothing in both time and scale. WTC reveals the time-frequency phase-locked behavior and thus it was used here to characterize the localized similarity between the two signals recorded from two brain regions. The Matlab package presented by [27] was used for the analysis.

C. Nonparametric Permutation Testing

Recorded ΔHbO_2 signals from each subject were divided into two segments: **Segment 1** and **Segment 2**, which included the time-courses corresponding to the first half and the second half of the number of total target trials, respectively. Nonparametric permutation testing, based on WTC values, was then used to test whether there is a significant difference in functional connectivity when assessed from time-courses in **Segment 1**, **Segment 2**, or the entire number of target trials. Compared to traditional parametric testing techniques which rely on assumptions about the shape of the distribution (e.g. a normal distribution), non-parametric statistical testings do not require assumptions about the shape or the parameters of the population distribution, thus they are appropriate to be used for datasets with unusual distributions [29]. The null-hypothesis here is that there is no difference in cross-coherence values when computed from time-courses in three difference cases (**Segment 1**, **Segment 2**, and the entire trials).

IV. RESULTS AND DISCUSSION

As stated previously, WTC was used to quantify the similarity between channel pairs. As a result, a series of scalograms, specifying the localized cross-coherence values for the time-courses of each channel pair were generated (see Fig. 2). The entire time-courses of ΔHbO_2 were used to generate the scalograms. Taking into account the ITI, the cross-coherence values in the frequency band of [0.08 Hz-0.1 Hz], where the "target" stimuli was presented to subjects, were considered for the similarity analysis. The mean cross-coherence values within this frequency band for the survived trials for each channel pair were then calculated as a measure of connectivity between the two channels. Across all subjects, 47 trials in **Segment 1**, and 36 trials in **Segment 2** survived the preprocessing step.
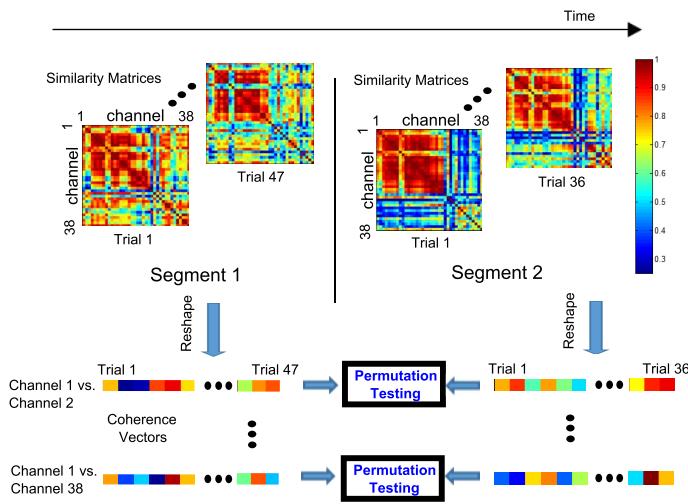
Fig. 3. Flowchart for the generation of coherence vectors for each channel-pair, from **Segment 1** and **Segment 2** respectively. These vectors are used for the permutation testing to examine whether there is a change in the similarities of channel-pairs in two cases.

Since there are 38 channels, this procedure generated a 38×38 similarity matrix for each trial. Coherence vectors including the mean cross-coherence values for all the survived trials for each channel-pair in each segment were then generated (see Fig. 3). Next, permutation testing were employed to test the statistical difference between connectivity for each channel-pair when assessed from **Segment 1** against when assessed from **Segment 2**. For this analysis, a relatively large number of iteration (1000), was considered.

The calculated p-values from the statistical test were used to form a 38×38 matrix. Values larger than 0.01 were set to zero. The remaining values were then utilized to construct the 3D maps of connections among different channels (Fig. 4-a). With $p < 0.01$, 102 channel-pairs presented significant difference in functional connectivity when assessed in two segments.

Additionally, a similar set of analysis was performed to compare the difference in functional connectivity when assessed from recordings of each segment and from the entire trials. The channel-pairs with significant changes ($p < 0.05$) in the similarity are visually illustrated in Fig. 4-b **Segment 1** vs. entire trials comparison, and in Fig. 4-c for **Segment 2** vs. entire trials comparison. 18 and 65 channel-pairs showed significant statistical differences in Fig. 4-b and Fig. 4-c, respectively. These results suggest that there may exist dynamic behaviors in the functional connectivity across the repeated trials of the same nature, and ignoring these changes will introduce bias in the conclusions of functional connections among brain networks.

REFERENCES

[1] S. Herculano-Houzel, "The human brain in numbers: a linearly scaled-up primate brain," *Frontiers in human neuroscience*, vol. 3, 2009.

[2] B. Biswal, F. Zerrin Yetkin, V. M. Haughton, and J. S. Hyde, "Functional connectivity in the motor cortex of resting human brain using echo-planar mri," *Magnetic resonance in medicine*, vol. 34, no. 4, pp. 537–541, 1995.
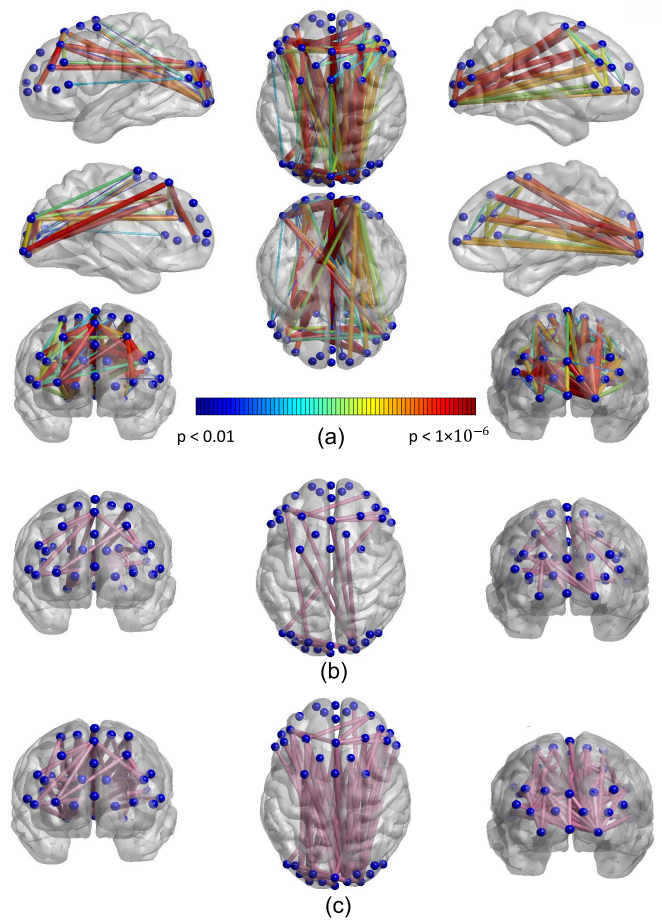
Fig. 4. Visual illustration of the statistical significance of the difference in channel-pair similarity when assessed in three scenarios [30]: (a) Segment 1 vs. Segment 2, (b) Segment 1 vs. whole duration, (c) Segment 2 vs. whole duration. $p < 0.05$ is used for (b) and (c). Blue points represent the location of channels.

[3] C. J. Honey, R. Kötter, M. Breakspear, and O. Sporns, "Network structure of cerebral cortex shapes functional connectivity on multiple time scales," *Proceedings of the National Academy of Sciences*, vol. 104, no. 24, pp. 10 240–10 245, 2007.

[4] K. J. Friston, "Functional and effective connectivity: a review," *Brain connectivity*, vol. 1, no. 1, pp. 13–36, 2011.

[5] Q. R. Razlighi, J. Steffener, C. Habeck, A. Laine, and Y. Stern, "Resting state inter and intra hemispheric human brain functional connectivity," in *35th Annual International Conference of the IEEE Engineering in Medicine and Biology Society (EMBC)*, 2013, pp. 6522–6525.

[6] N. Karamzadeh, A. Medvedev, A. Azari, A. Gandjbakhche, and L. Najafizadeh, "Capturing dynamic patterns of task-based functional connectivity with eeg," *NeuroImage*, vol. 66, pp. 311–317, 2013.

[7] L.-L. Zeng, H. Shen, L. Liu, L. Wang, B. Li, P. Fang, Z. Zhou, Y. Li, and D. Hu, "Identifying major depression using whole-brain functional connectivity: a multivariate pattern analysis," *Brain*, p. aws059, 2012.

[8] J. M. Tyszka, D. P. Kennedy, L. K. Paul, and R. Adolphs, "Largely typical patterns of resting-state functional connectivity in high-functioning adults with autism," *Cerebral Cortex*, p. bht040, 2013.

[9] A. M. Mishra, X. Bai, B. G. Sanganahalli, S. G. Waxman, O. Shatillo, O. Grohn, F. Hyder, A. Pitkänen, and H. Blumenfeld, "Decreased resting functional connectivity after traumatic brain injury in the rat," *PloS one*, vol. 9, no. 4, p. e95280, 2014.

[10] A. V. Medvedev, "Does the resting state connectivity have hemispheric asymmetry? a near-infrared spectroscopy study," *NeuroImage*, vol. 85, pp. 400–407, 2014.

[11] B. R. White, S. M. Liao, S. L. Ferradal, T. E. Inder, and J. P. Culver, "Bedside optical imaging of occipital resting-state functional connectivity in neonates," *Neuroimage*, vol. 59, no. 3, pp. 2529–2538,

2012.

[12] V. D. Calhoun, V. K. Potluru, R. Phlypo, R. F. Silva, B. A. Pearlmutter, A. Caprihan, S. M. Plis, and T. Adalı, "Independent component analysis for brain fmri does indeed select for maximal independence," *PloS one*, vol. 8, no. 8, p. e73309, 2013.

[13] C. Chang and G. H. Glover, "Time–frequency dynamics of resting-state brain connectivity measured with fmri," *Neuroimage*, vol. 50, no. 1, pp. 81–98, 2010.

[14] X.-S. Hu, K.-S. Hong, and S. S. Ge, "Reduction of trial-to-trial variability in functional near-infrared spectroscopy signals by accounting for resting-state functional connectivity," *Journal of biomedical optics*, vol. 18, no. 1, pp. 017 003–017 003, 2013.

[15] M. D. Fox, A. Z. Snyder, J. M. Zacks, and M. E. Raichle, "Coherent spontaneous activity accounts for trial-to-trial variability in human evoked brain responses," *Nature neuroscience*, vol. 9, no. 1, pp. 23–25, 2005.

[16] M. D. Fox, A. Z. Snyder, J. L. Vincent, and M. E. Raichle, "Intrinsic fluctuations within cortical systems account for intertrial variability in human behavior," *Neuron*, vol. 56, no. 1, pp. 171–184, 2007.

[17] F. Amyot, T. Zimmermann, J. Riley, J. M. Kainerstorfer, V. Chernomordik, E. Mooshagian, L. Najafizadeh, F. Krueger, A. H. Gandjbakhche, and E. M. Wassermann, "Normative database of judgment of complexity task with functional near infrared spectroscopyapplication for tbi," *Neuroimage*, vol. 60, no. 2, pp. 879–883, 2012.

[18] M. Ferrari and V. Quaresima, "A brief review on the history of human functional near-infrared spectroscopy (fnirs) development and fields of application," *Neuroimage*, vol. 63, no. 2, pp. 921–935, 2012.

[19] L. Zhu, M. Peifer, and L. Najafizadeh, "Towards improving the"detection" power of brain imaging experiments using fnirs," in *Biomedical Optics*. Optical Society of America, 2014, pp. BM3A–29.

[20] L. Wang, Y. Kuroiwa, T. Kamitani, T. Takahashi, Y. Suzuki, and O. Hasegawa, "Effect of interstimulus interval on visual p300 in parkinsons disease," *Journal of Neurology, Neurosurgery & Psychiatry*, vol. 67, no. 4, pp. 497–503, 1999.

[21] T. Ozawa, T. Aihara, Y. Fujiwara, Y. Otaka, I. Nambu, R. Osu, J. Izawa, and Y. Wada, "Detecting event-related motor activity using functional near-infrared spectroscopy," in *6th International IEEE/EMBS Conference on Neural Engineering (NER)*, 2013, pp. 1529–1532.

[22] A. Bozkurt, A. Rosen, H. Rosen, and B. Onaral, "A portable near infrared spectroscopy system for bedside monitoring of newborn brain," *Biomedical engineering online*, vol. 4, no. 1, p. 29, 2005.

[23] G. Taga, H. Watanabe, and F. Homae, "Spatiotemporal properties of cortical haemodynamic response to auditory stimuli in sleeping infants revealed by multi-channel near-infrared spectroscopy," *Philosophical Transactions of the Royal Society A: Mathematical, Physical and Engineering Sciences*, vol. 369, no. 1955, pp. 4495–4511, 2011.

[24] C. Torrence and G. P. Compo, "A practical guide to wavelet analysis," *Bulletin of the American Meteorological society*, vol. 79, no. 1, pp. 61–78, 1998.

[25] Q. Yang, V. Siemionow, W. Yao, V. Sahgal, and G. H. Yue, "Single-trial eeg-emg coherence analysis reveals muscle fatigue-related progressive alterations in corticomuscular coupling," *Neural Systems and Rehabilitation Engineering, IEEE Transactions on*, vol. 18, no. 2, pp. 97–106, 2010.

[26] A. Klein, T. Sauer, A. Jedynak, and W. Skrandies, "Conventional and wavelet coherence applied to sensory-evoked electrical brain activity," *Biomedical Engineering, IEEE Transactions on*, vol. 53, no. 2, pp. 266–272, 2006.

[27] A. Grinsted, J. C. Moore, and S. Jevrejeva, "Application of the cross wavelet transform and wavelet coherence to geophysical time series," *Nonlinear processes in geophysics*, vol. 11, no. 5/6, pp. 561–566, 2004.

[28] C. Torrence and P. J. Webster, "Interdecadal changes in the enso-monsoon system," *Journal of Climate*, vol. 12, no. 8, pp. 2679–2690, 1999.

[29] E. Maris and R. Oostenveld, "Nonparametric statistical testing of eeg-and meg-data," *Journal of neuroscience methods*, vol. 164, no. 1, pp. 177–190, 2007.

[30] M. Xia, J. Wang, and Y. He, "Brainnet viewer: a network visualization tool for human brain connectomics," *PLoS One*, vol. 8, no. 7, p. e68910, 2013.